

# Posterodorsal Medial Amygdala Urocortin-3, GABA, and Glutamate Mediate Suppression of LH Pulsatility in Female Mice

Deyana Ivanova,<sup>1</sup>  Xiao-Feng Li,<sup>1</sup> Caitlin McIntyre,<sup>1</sup> and Kevin T. O'Byrne<sup>1</sup> 

<sup>1</sup>Department of Women and Children's Health, School of Life Course and Population Sciences, Faculty of Life Science and Medicine, King's College London, London SE1 1UL, UK

**Correspondence:** Deyana Ivanova, PhD, Department of Women and Children's Health, School of Life Course and Population Sciences, Faculty of Life Science and Medicine, King's College London, 2.92W Hodgkin Building, Guy's Campus, London SE1 1UL, UK. Email: [deyana.ivanova@kcl.ac.uk](mailto:deyana.ivanova@kcl.ac.uk); or Kevin T. O'Byrne, PhD, Department of Women and Children's Health, School of Life Course and Population Sciences, Faculty of Life Science and Medicine, King's College London, 2.92W Hodgkin Building, Guy's Campus, London SE1 1UL, UK. Email: [kevin.obyrne@kcl.ac.uk](mailto:kevin.obyrne@kcl.ac.uk).

## Abstract

The posterodorsal subnucleus of the medial amygdala (MePD) is an upstream modulator of the hypothalamic–pituitary–gonadal (HPG) and hypothalamic–pituitary–adrenal (HPA) axes. Inhibition of MePD urocortin-3 (Ucn3) neurons prevents psychological stress–induced suppression of luteinizing hormone (LH) pulsatility while blocking the stress-induced elevations in corticosterone (CORT) secretion in female mice. We explore the neurotransmission and neural circuitry suppressing the gonadotropin-releasing hormone (GnRH) pulse generator by MePD Ucn3 neurons and we further investigate whether MePD Ucn3 efferent projections to the hypothalamic paraventricular nucleus (PVN) control CORT secretion and LH pulsatility. Ucn3-cre-tdTomato female ovariectomized (OVX) mice were unilaterally injected with adeno-associated virus (AAV)-channelrhodopsin 2 (ChR2) and implanted with optofluid cannulae targeting the MePD. We optically activated Ucn3 neurons in the MePD with blue light at 10 Hz and monitored the effect on LH pulses. Next, we combined optogenetic stimulation of MePD Ucn3 neurons with pharmacological antagonism of GABA<sub>A</sub> or GABA<sub>B</sub> receptors with bicuculline or CGP-35348, respectively, as well as a combination of NMDA and AMPA receptor antagonists, AP5 and CNQX, respectively, and observed the effect on pulsatile LH secretion. A separate group of Ucn3-cre-tdTomato OVX mice with 17 $\beta$ -estradiol replacement were unilaterally injected with AAV-ChR2 in the MePD and implanted with fiber-optic cannulae targeting the PVN. We optically stimulated the MePD Ucn3 efferent projections in the PVN with blue light at 20 Hz and monitored the effect on CORT secretion and LH pulses. We reveal for the first time that activation of Ucn3 neurons in the MePD inhibits GnRH pulse generator frequency via GABA and glutamate signaling within the MePD, while MePD Ucn3 projections to the PVN modulate the HPG and HPA axes.

**Key Words:** Ucn3, GABA, glutamate, MePD, PVN, LH pulsatility, CORT secretion

**Abbreviations:** AAV, adeno-associated virus; AMPA,  $\alpha$ -amino-3-hydroxy-5-methyl-4-isoxazole propionic acid; ARC, arcuate nucleus; BIC, bicuculline; ChR2, channelrhodopsin 2; CRF, corticotropin-releasing factor; E<sub>2</sub>, 17 $\beta$ -estradiol; CORT, corticosterone; GABA,  $\gamma$ -aminobutyric acid; GnRH, gonadotropin-releasing hormone; HPA, hypothalamic–pituitary–adrenal; HPG, hypothalamic–pituitary–gonadal; kiss1, kisspeptin; LH, luteinizing hormone; MePD, medial amygdala; NMDA, N-methyl-D-aspartate; OVX, ovariectomized; PVN, paraventricular nucleus; Ucn3, urocortin-3.

Stress exerts a profound suppressive effect on reproduction in mammals, including rodents and humans. The amygdala, part of the limbic system, is a key emotional center integrating incoming cues from the external environment, such as anxiogenic signals, with the reproductive and stress axes (1). The posterodorsal subnucleus of the medial amygdala (MePD) is an upstream modulator of pulsatile luteinizing hormone (LH) secretion (2–4), and exerts an inhibitory break on pubertal timing (5, 6). The MePD sends direct projections, of an unknown phenotype, to the kisspeptin (kiss1) neuronal population in the hypothalamic arcuate nucleus (ARC) (7, 8) known as KNDy because they coexpress neurokinin B and dynorphin A (Dyn) (9–11). The synchronous activity of the ARC KNDy network drives pulsatile gonadotropin-releasing hormone (GnRH) and LH release (11–14). The MePD also contains a kiss1 neuronal population, and

selective optogenetic activation of these neurons increases GnRH pulse generator frequency in mice (3); unpublished observations show this is an effect involving both MePD GABA and glutamate signaling.

We have recently shown that urocortin-3 (Ucn3), a member of the corticotropin-releasing factor (CRF) stress neuropeptide family, and its receptor CRF type 2 (CRFR2) signaling in the MePD are involved in mediating the suppressive effect of psychosocial stress on LH pulsatility (4). However, the underlying neural mechanisms involved in mediating the inhibitory effect of MePD Ucn3 neurons on LH pulsatility remain to be established. GABA ( $\gamma$ -aminobutyric acid) and glutamate signaling in the amygdala are implicated in the modulation of anxiety behavior (15, 16). The amygdala also modulates the stress response through the hypothalamic–pituitary–adrenal (HPA) axis. The medial amygdala activates the

HPA axis in response to predator odor stress (17), and the MePD in particular has been shown to send stress-activated efferents to the paraventricular nucleus of hypothalamus (PVN) (18). Furthermore, MePD Ucn3 and CRFR2-positive neurons are implicated in regulating the stress response, with restraint stress increasing MePD Ucn3 (19) and social defeat elevating MePD CRFR2 expression in rodents (20). Moreover, MePD Ucn3 and CRFR2-positive neurons project to the PVN (21), and we have recently shown that chemogenetic inhibition of MePD Ucn3 neurons prevents psychogenic stress-induced corticosterone (CORT) release in female mice (4).

In this study, we aimed to determine whether activation of MePD Ucn3 neurons inhibits pulsatile LH secretion via GABA and/or glutamate signaling within this amygdala subnucleus. To achieve this, we will combine selective optogenetic activation of MePD Ucn3 neurons with pharmacological antagonism of GABA<sub>A</sub> or GABA<sub>B</sub> receptors, or a combination of N-methyl-D-aspartate (NMDA) and  $\alpha$ -amino-3-hydroxy-5-methyl-4-isoxazole propionic acid (AMPA) receptors, respectively, using chronically implanted intra-MePD optofluid cannulae while collecting serial blood samples for LH pulse measurement in Ucn3-Cre-tdTomato female mice. Additionally, we will investigate whether optogenetic stimulation of MePD Ucn3 projection terminals in the PVN induce CORT release and suppress LH pulsatility.

## Materials and Methods

### Mice

Cryopreserved sperm of Ucn3-cre mice (strain Tg(Ucn3-cre)KF43Gsat/Mmucd; congenic on C57BL/6 background) was acquired from MMRRRC GENSAT and heterozygous transgenic breeding pairs of Ucn3-Cre mice were recovered via insemination of female C57Bl6/J mice at King's College London, as described previously (4). Ucn3-Cre mice were genotyped using polymerase chain reaction for the detection of heterozygosity, and Ucn3-cre mice were bred with tdTomato mice (strain B6.Cg-Gt(ROSA)26Sortm9(CAG-tdTomato)Hze/J; congenic on C57BL/6 background) acquired from the Jackson Laboratory (Bar Harbor, ME, USA) to produce Ucn3-cre-tdTomato reporter mice, as described previously (4, 21). Female Ucn3-cre-tdTomato mice weighing 19 to 23 g and aged 6-8 weeks were singly housed in individually ventilated cages sealed with a HEPA filter at  $25 \pm 1$  °C in a 12:12 hours light/dark cycle, lights on at 07:00 hours equipped with nesting material, woodchip bedding, and food and water ad libitum. All procedures were carried out following the United Kingdom Home Office Regulations and approved by the Animal Welfare and Ethical Review Body Committee at King's College London.

### Stereotaxic Injection of Adeno-Associated Virus Carrying the Channelrhodopsin Construct and Fiber-Optic or Optofluid Cannula Implantation

All surgical procedures were carried out under aseptic conditions with general anesthesia using ketamine (Vetalar, 100 mg/kg, intraperitoneally; Pfizer, Sandwich, UK) and xylazine (Rompun, 10 mg/kg, intraperitoneally; Bayer, Leverkusen, Germany). Ucn3-Cre-tdTomato mice were secured in a David Kopf stereotaxic frame (Kopf Instruments, Model 900) and either solely bilaterally ovariectomized (OVX) or implanted with a

17 $\beta$ -estradiol (E<sub>2</sub>) silastic capsule. E<sub>2</sub> was dissolved in sesame oil to reach a final concentration of 36  $\mu$ g E<sub>2</sub>/mL and filled into 14-mm capsules of inner/outer diameter 1.575/3.175 mm, as previously described (22). The reference study reported that at 21 days of implantation, serum E<sub>2</sub> concentrations were within physiological concentrations equivalent to those found in mice in the diestrous stage of the cycle. However, by 35 days of implantation the serum E<sub>2</sub> concentrations had slowly declined but were still within the range found in diestrous mice. Due to the technically demanding nature of our experiments, the E<sub>2</sub> capsules were implanted for longer than 35 days after surgery during the experimental period. Therefore, E<sub>2</sub> levels may be lower than expected for the diestrous phase. E<sub>2</sub> is known to enhance the suppressive effects of stress where the action of the gonadal steroids sensitizes the HPA axis and augments stress-induced inhibition of the GnRH pulse generator in many species, from rodents to primates (23-26). We had 2 experimental groups: OVX only and OVX + E<sub>2</sub> capsule. The mouse brain atlas of Paxinos and Franklin (27) was used to obtain target coordinates for the MePD (2.29 mm lateral, -1.40 mm from bregma, at a depth of -5.42 mm below the skull surface). To reveal the skull, an incision was made in the scalp and 1 small hole was drilled above the location of the right MePD. AAV9-EF1a-double floxed-hChR2(H134R)-EYFP-WPRE-HGHpA (300 nL;  $3 \times 10^{11}$  GC/mL; Serotype:9; Addgene, MA, USA) was unilaterally injected into the right MePD using a 2- $\mu$ L Hamilton microsyringe (Esslab, Essex, UK) over 10 minutes, using the robot stereotaxic system (Neurostar, Tubingen, Germany), performed for the targeted expression of ChR2-EYFP in MePD Ucn3 neurons. After injection, the needle was left in position for a further 5 minutes and lifted slowly over 2 minutes. Cre-positive mice received the adeno-associated virus (AAV)-channelrhodopsin 2 (ChR2) injection (test mice) or a control virus AAV-YFP (Addgene) (control mice). The control virus does not contain the ChR2 construct. The mice were then implanted with a dual optofluid cannula (Doric Lenses, Quebec, Canada) at the same anterior-posterior and medial-lateral coordinates as the viral injection site; however, a different dorsal-ventral was used such that the internal cannula targets the MePD and the optofluid cannula is situated 0.2 mm above the MePD site. Once in position, the optofluid cannula was secured on the skull using dental cement (Super-Bond Universal Kit, Prestige Dental, UK), and the incision of the skin was closed with suture. Mice were left to recover for 1 week and after the recovery period, mice were handled daily to acclimatize to experimental procedures for a further 2 weeks. Thirteen mice received the AAV-ChR2 injection and were implanted with an optofluid cannula in the MePD. Five mice received the control AAV-YFP and were implanted with an optofluid cannula in the MePD. Eleven mice received the AAV-ChR2 injection in the MePD and were implanted with an optic fiber in the PVN. Five mice received the control AAV-YFP and were implanted with an optic fiber in the PVN.

### In Vivo Optogenetic Stimulation of MePD Urocortin-3 Neurons

To test the effect of optogenetic stimulation of MePD Ucn3 neurons on LH pulsatility, the ferrule of the implanted optofluid cannula, on the right side of the MePD, was attached via a ceramic mating sleeve to a multimode fiber-optic rotary joint patch cable (Thorlabs Ltd, Ely, UK) at a length allowing for free movement of the mice in their cage, and blue light (473 nm wavelength; 10 mW) was delivered using a

Grass SD9B stimulator-controlled laser (Laserglow Technologies, Toronto, Canada). The mice were left to acclimatize for 1 hour. Following the acclimatization period, blood samples (5  $\mu$ L) were collected every 5 minutes for 2 hours. After 1 hour of control blood sampling, Ucn3-cre-tdTomato mice received optic stimulation at 10 Hz with a 10-ms pulse interval and pattern stimulation of 5 seconds on and 5 seconds off for the remaining 1 hour.

### Intra-MePD Administration of Bicuculline, CGP-35348, or AP5 + CNQX During Optogenetic Stimulation of MePD Urocortin-3 Neurons

Neuropharmacological manipulation of GABA and glutamate receptor signaling in the MePD with or without optogenetic stimulation of MePD Ucn3 neurons was done to test whether MePD Ucn3-induced suppression of LH pulsatility involves GABA or glutamate receptor signaling. OVX mice implanted with an optofluid cannula in the MePD were subjected to the tail-tip blood collection procedure, as previously described (28). Infusion of drugs with or without optogenetic stimulation and blood sampling were performed between 09:00 and 13:00 hours, where 5  $\mu$ L of blood was collected every 5 minutes for 2 hours. An internal cannula (Doric Lenses) attached to extension tubing (0.58 mm ID, 0.96 mm OD), preloaded with bicuculline (BIC) (GABA<sub>A</sub> receptor antagonist; Sigma-Aldrich), CGP-35348 (GABA<sub>B</sub> receptor antagonist; Sigma-Aldrich), AP5 + CNQX cocktail (NMDA and AMPA receptor antagonists; Tocris), or aCSF as vehicle control, was inserted into the guide cannula of the optofluid implant and mice were connected to the laser, as described above. The tubing for drug infusion extended beyond the cage and the distal ends were attached to 10- $\mu$ L Hamilton syringes (Waters Ltd, Elstree, UK) fitted into a PHD 2000 Programmable syringe pump (Harvard Apparatus, MA, USA), allowing for a continuous infusion of the drug at a constant rate; mice were kept in the cage throughout the experiment, freely moving with food and water ad libitum. After 55 minutes of control blood sampling, the mice were given an initial bolus injection, 0.30  $\mu$ L at a rate of 0.06  $\mu$ L/minutes over 5 minutes, of BIC, CGP-35348, AP5 + CNQX, or aCSF. The laser was turned on at 60 minutes and the bolus injection was followed by a continuous infusion, 0.8  $\mu$ L at a rate of 0.01  $\mu$ L/minute over 1 hour, of BIC, CGP-35348, AP5 + CNQX, or aCSF. BIC, CGP-35348, AP5, and CNQX were dissolved in aCSF to reach bolus concentrations of 20 pmol, 4.5 nmol, 1.2, and 0.5 nmol, respectively. The concentrations for the continuous infusion of BIC, CGP-35348, AP5, and CNQX were 68 pmol, 15, 2, and 1 nmol, respectively. In the absence of optic stimulation, the same regimen was applied. Data collection was conducted over a period of 4 to 6 weeks. The mice received all treatments in a random order, with at least 2 days between experiments.

### MePD Urocortin-3 Terminal Optogenetic Stimulation in the PVN

To test the effect of optogenetic stimulation of MePD Ucn3 neuronal terminals in the PVN on LH pulsatility and CORT release, OVX + E<sub>2</sub> Ucn3-cre-tdTomato mice with AAV-ChR2 injection in the right MePD implanted with a fiber-optic cannula in the right PVN were subjected to the tail-tip blood collection procedure, as previously described (28). For LH measurement, blood samples were collected every 5 minutes for 2 hours, as described

above. Mice were connected to the laser, as described above. Optogenetic stimulation was initiated after the 1-hour control blood sampling period, and Ucn3-cre-tdTomato mice received optic stimulation at 20 Hz, 15 mW with a 10-ms pulse interval and pattern stimulation of 5 seconds on and 5 seconds off for the remaining 1 hour. For CORT measurements, 15- $\mu$ L blood samples were collected on a separate occasion, and blood samples were stored in tubes containing 5  $\mu$ L of heparinized saline (5 IU/mL). Optogenetic stimulation was initiated, as described above, 30 minutes into the experiment (time point, 0 minutes) and lasted for 1 hour (time point 60 minutes). Remaining blood samples were collected at 0, 30, and 60 minutes, with a final sample taken 1 hour after the termination of optogenetic stimulation (time point, 120 minutes). At the end of the experiment, blood samples were centrifuged at 13 000 RPM for 20 minutes at 20 °C and plasma was stored at -20 °C. Data collection was conducted over a period of 4 to 6 weeks. All experiments were performed between 9:00 and 12:00 hours.

### Validation of AAV Injection and Cannula Implant Site

Upon completion of experiments, mice were anaesthetized with a lethal dose of ketamine and transcatheterial perfusion was performed with heparinized saline for 5 minutes followed by ice-cold 4% paraformaldehyde in phosphate buffer (pH 7.4) for 15 minutes using a pump (Minipuls, Gilson, Villiers Le Bel, France). Mice brains were collected immediately and postfixed in 15% sucrose in 4% paraformaldehyde at 4 °C and left to sink. Once sunk, they were transferred to 30% sucrose in phosphate-buffered saline and left to sink. Brains were snap-frozen in isopropanol on dry ice and stored in -80 °C until further processing. Every third coronal brain section (30  $\mu$ m/section) throughout the MePD region (-1.34 mm to -2.70 mm from bregma) was collected using a cryostat (Bright Instrument Co., Luton, UK). Sections were mounted on microscope slides, air dried, and covered with ProLong Antifade mounting medium (Molecular Probes, Inc., OR, USA). Cannula placement and AAV injection site were verified with Axioskop 2 Plus microscope equipped with Axiovision, version 4.7 (Zeiss) by determining whether the cannulae reach the MePD. For AAV-ChR2-EYFP-injected Ucn3-cre-tdTomato mice we determined whether Ucn3 neurons were infected in the MePD region by merging td-Tomato fluorescence of Ucn3 neurons with YFP fluorescence in the MePD. The number of Ucn3 YFP-positive neurons colocalized with td-Tomato fluorescence in the MePD of each animal was counted using 4 sections, and the average number of neurons presented is per section per MePD. The group mean percent was calculated by taking the average number of Ucn3 YFP-positive neurons out of the average number of Ucn3 neurons expressing td-Tomato fluorescence per 4 sections and presented as mean  $\pm$  SEM %, as described previously (4). An Axioskop 2 Plus microscope (Carl Zeiss) equipped with axiovision, version 4.7 (Carl Zeiss), was used to take images. Only mice with the correct AAV injection and cannula placement in the MePD were analyzed.

### LH and CORT Measurement

Mice were handled daily to acclimatize to the tail-tip blood sampling procedure for LH measurement (4). Blood samples collected for LH measurement were processed using LH enzyme-linked immunosorbent assay, as previously reported

(4). The capture antibody (monoclonal antibody, anti-bovine LH $\beta$  subunit, RRID:AB\_2665514) was purchased from Department of Animal Science at the University of California, Davis. The mouse LH standard (AFP-5306A) and primary antibody (polyclonal antibody, rabbit LH anti-serum, RRID:AB\_2665533) were obtained from Harbour-UCLA (CA, USA). The secondary antibody (horse-radish peroxidase-linked donkey anti-rabbit IgG polyclonal antibody, RRID:AB\_772206) was purchased from VWR International (Leicestershire, UK). Intra-assay and interassay variations were 4.6% and 10.2%, respectively, and the assay sensitivity was 0.0015 ng/mL. The DynPeak algorithm was used for the detection of LH pulses (4). The effect of optogenetic stimulation of MePD Ucn3 neurons and neuropharmacology studies was established by comparing the LH interspike interval from the 1-hour control period (prestimulation) or drug administration control period to the 1-hour experimental period, as previously described (4). The LH pulse amplitude was calculated as the difference between the peak of an LH pulse and the baseline LH level before the onset of the pulse. The means were compared between the pretreatment and treatment periods for all experiments. The LH pulse amplitude was also compared between experimental groups within the treatment period. The mean LH value for each LH pulse profile was quantified by summing all values from 1 LH pulse profile and dividing by the number of values recorded in 120 minutes.

Blood samples were collected for CORT measurement were processed using a commercially available enzyme immunoassay kit (sheep polyclonal antibody specific for CORT, RRID:AB\_2877626; DetectX Corticosterone Enzyme Immunoassay Kit, K014; Arbor Assays, MI, USA), as described previously (4).

## Statistics

Mice were compared between groups using a 2-way analysis of variance with a Tukey post hoc. Data are presented as mean  $\pm$  SEM. Statistics were performed using Igor Pro 7 (Wavemetrics, Lake Oswego, OR, USA). Data are presented as mean  $\pm$  SEM.  $P < .05$ ,  $P < .001$ , and  $P < .0001$  were considered to be statistically significant.

## Results

### Effects of Optogenetic Stimulation of MePD Urocortin-3 Neurons on LH Pulse Frequency

Optogenetic stimulation of MePD Ucn3 neurons in control mice had no effect on LH pulse interval (Fig. 1A; AAV-YFP:  $n = 3$ ), and administration of aCSF alone (AAV-YFP with no stimulation:  $n = 2$ ) had no effect on LH pulse interval. Optogenetic stimulation of MePD Ucn3 neurons with blue light at 10 Hz, 10 mW suppressed pulsatile LH secretion (Fig. 1B; AAV-ChR2:  $n = 9$ ). These data are summarized in Fig. 1C. LH pulse amplitude and mean LH levels were quantified and data are provided in Table 1.

### Effects of Intra-MePD Administration of BIC, a GABA<sub>A</sub>R Antagonist, and CGP, a GABA<sub>B</sub>R Antagonist, During Optical Stimulation of MePD Urocortin-3 Neurons on LH Pulsatility

Delivery of BIC alone had no significant effect on LH pulsatility (Fig. 1D;  $n = 8$ ). Intra-MePD infusion of BIC during

optogenetic stimulation of MePD Ucn3 neurons with blue light at 10 Hz, 10 mW completely blocked the suppressive effect of MePD Ucn3 neuronal activation on LH pulsatility (Fig. 1E;  $n = 9$ ). The results of this experiment are summarized in Fig. 1F. LH pulse amplitude and mean LH levels were quantified and data are provided in Table 1.

### Effects of Intra-MePD Administration of CGP, a GABA<sub>B</sub>R Antagonist, During Optical Stimulation of MePD Urocortin-3 Neurons on LH Pulsatility

Delivery of CGP alone had no significant effect on LH pulsatility (Fig. 1G;  $n = 7$ ). Intra-MePD infusion of CGP during optogenetic stimulation of MePD Ucn3 neurons with blue light at 10 Hz, 10 mW completely blocked the suppressive effect of MePD Ucn3 neuronal activation on LH pulsatility (Fig. 1H;  $n = 7$ ). The results of this experiment are summarized in the Fig. 1I. LH pulse amplitude and mean LH levels were quantified and data are provided in Table 1.

### Effects of Intra-MePD Glutamate Antagonism During Optogenetic Stimulation of MePD Urocortin-3 Neurons on LH Pulsatility

Delivery of AP5 (selective NMDA antagonist) + CNQX (selective AMPA antagonist) alone had no significant effect on LH pulsatility (Fig. 1J;  $n = 6$ ). Intra-MePD infusion of AP5 + CNQX during optogenetic stimulation of MePD Ucn3 neurons with blue light at 10 Hz, 10 mW completely blocked the suppressive effect of MePD Ucn3 neuronal activation on LH pulsatility (Fig. 1K;  $n = 6$ ). The results of this experiment are summarized in the Fig. 1L. LH pulse amplitude and mean LH levels were quantified and data are provided in Table 1.

### Effect of MePD Urocortin-3 Terminal Stimulation in the PVN on Dynamic CORT Secretion

Optogenetic stimulation of MePD Ucn3 neuron terminals in the PVN with blue light at 20 Hz, 15 mW elevated CORT secretion compared with controls (Fig. 2; AAV-ChR2:  $n = 6$ ). Optogenetic stimulation of MePD Ucn3 neurons and terminal projections in the PVN of control mice had no effect on dynamic CORT secretion (AAV-YFP;  $n = 5$ ).

### Effect of MePD Urocortin-3 Terminal Stimulation in the PVN on LH Pulsatility

Optogenetic stimulation of MePD Ucn3 projections in the PVN of control mice had no effect on LH pulse interval (Fig. 3A and 3C; AAV-YFP,  $n = 3$ ; wild-type with AAV-ChR2,  $n = 2$ ) and no stimulation of the MePD Ucn3 projections in the PVN (no stimulation,  $n = 2$ ) had any effect on LH pulse interval. Optogenetic stimulation of MePD Ucn3 neuron terminals in the PVN with blue light at 20 Hz, 15 mW reduced LH pulsatility compared with controls (Fig. 3B and 3D; AAV-ChR2:  $n = 8$ ). These data are summarized in Fig. 3E. LH pulse amplitude and mean LH levels were quantified and data are provided in Table 2.

### Selective Expression of ChR2 in MePD Ucn3 Neurons and MePD Ucn3 Neuron Projections in the PVN, and Validation of Cannula Position

Evaluation of AAV9-EF1a-double floxed-hChR2(H134R)-EYFP-WPRE-HGHpA expression in tdTomato-labeled

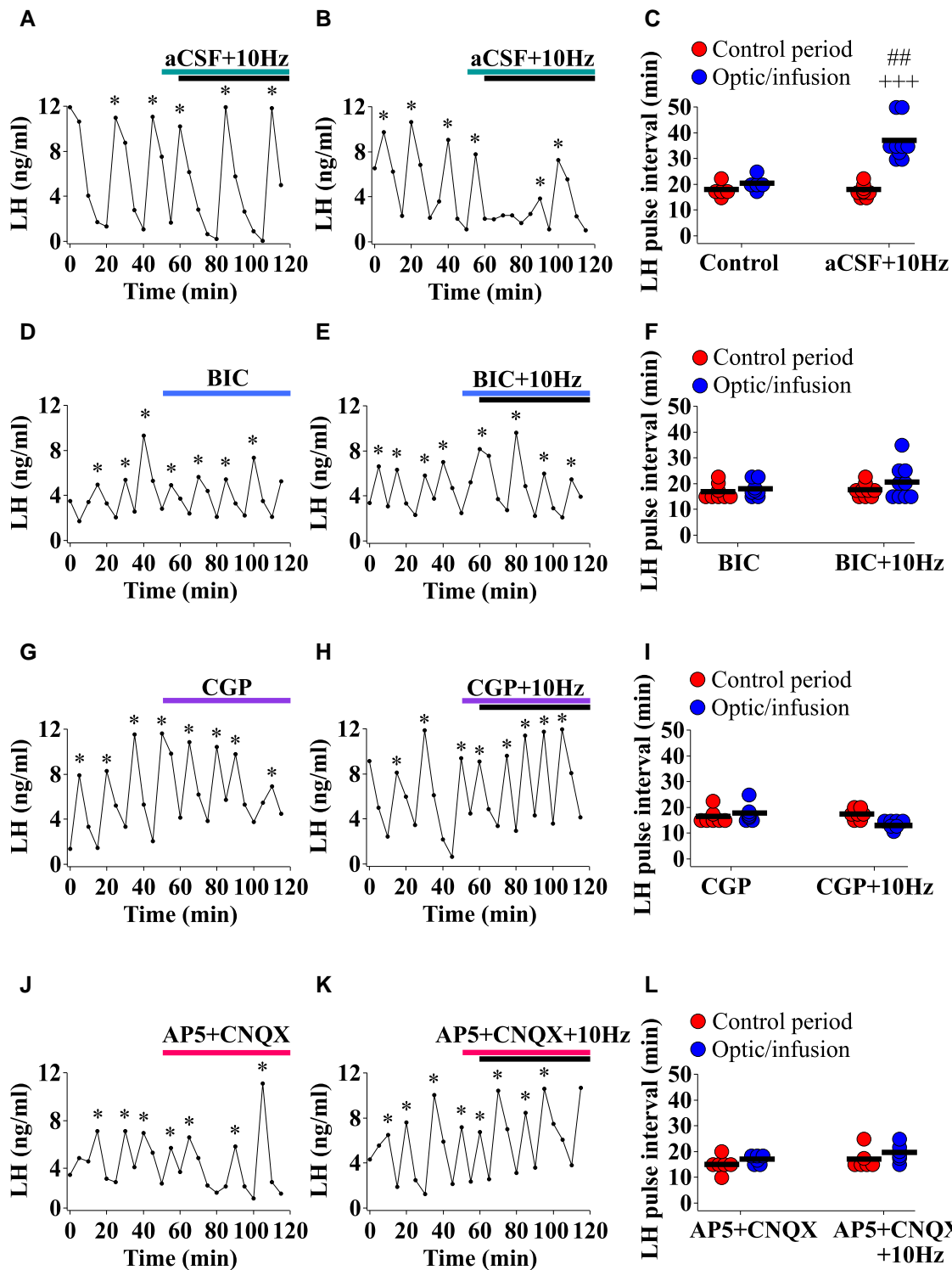


**Figure 1.** Optogenetic stimulation of posterodorsal medial amygdala (MePD) urocortin-3 (Ucn3) neurons with blue light at 10 Hz, 10 mW suppressed pulsatile LH secretion in adult ovariectomized Ucn3-cre-tdTomato female mice. Infusion of bicuculline (BIC), GABA<sub>A</sub> receptor antagonist, CGP, GABA<sub>B</sub> receptor antagonist, and AP5 and CNQX, NMDA and AMPA receptor antagonists, respectively, into the MePD during optogenetic stimulation of MePD Ucn3 neurons with blue light at 10 Hz, 10 mW completely blocked the suppressive effect of MePD Ucn3 neuronal activation on LH pulsatility. Representative LH pulse profiles showing the effects of (A) control AAV-YFP mice administered with aCSF receiving optical stimulation of 10 Hz, 10 mW. (B) AAV-ChR2 mice administered with aCSF receiving optical stimulation of 10 Hz, 10 mW. (C) Summary of LH pulse interval for the prestimulation control period (1 hour) and optical stimulation/infusion period (1 hour), (D) AAV-ChR2 mice administered with BIC. (E) AAV-ChR2 mice administered with BIC receiving optical stimulation of 10 Hz, 10 mW. (F) Summary of LH pulse interval. (G) AAV-ChR2 mice administered with CGP. (H) AAV-ChR2 mice administered with CGP receiving optical stimulation of 10 Hz, 10 mW. (I) Summary of LH pulse interval. (J) AAV-ChR2 mice administered with a combination of AP5 and CNQX. (K) AAV-ChR2 mice administered with a combination of AP5 and CNQX receiving optical stimulation of 10 Hz, 10 mW. (L) Summary of LH pulse interval. LH pulses detected by the DynPeak algorithm are indicated with an asterisk located above each pulse on the representative LH pulse profiles. For A-C +++*P* < .0001 control period vs optic stimulation + aCSF (AAV-ChR2: *n* = 9); ##*P* < .001 optic stimulation vs control group (AAV-YFP: *n* = 3; no stimulation: *n* = 2). For D-F *n* = 8 or 9 per group. For G-I *n* = 7 per group. For J-L *n* = 6 per group.

**Table 1. LH pulse amplitude and mean LH levels before and during simultaneous optogenetic stimulation with pharmacological manipulation of Ucn3 neurons in the posterodorsal subnucleus of the MePD in ovariectomized Ucn3-cre-tdTomato female mice**

Treatment	Mean LH pulse amplitude (ng/mL)		Mean LH level (ng/mL)	
	Pretreatment	Treatment	Pretreatment	Treatment
Control	8.07 ± 0.66	8.59 ± 1.03	6.57 ± 0.69	6.13 ± 0.78
Ucn3 optic stimulation 10 Hz + aCSF	7.63 ± 0.68	2.85 ± 0.51 <sup>a</sup>	6.02 ± 0.50	3.08 ± 0.34 <sup>a</sup>
BIC	6.55 ± 0.68	7.56 ± 0.86	4.88 ± 0.49	4.96 ± 0.25
Ucn3 optic stimulation 10 Hz + BIC	6.35 ± 0.59	7.52 ± 0.92	5.33 ± 0.61	5.17 ± 0.47
CGP	7.64 ± 1.17	7.10 ± 0.92	5.65 ± 0.73	5.94 ± 0.41
Ucn3 optic stimulation 10 Hz + CGP	8.15 ± 1.09	8.64 ± 0.65	6.47 ± 0.93	6.22 ± 0.70
AP5 + CNQX	5.93 ± 0.30	5.80 ± 0.40	4.15 ± 0.34	4.17 ± 0.40
Ucn3 optic stimulation 10 Hz + AP5 + CNQX	5.94 ± 0.60	5.83 ± 0.83	4.60 ± 0.57	5.53 ± 1.03

Data are presented as mean ± SEM. The LH pulse amplitude and mean LH levels of the treatment group for the Ucn3 optic stimulation 10Hz + aCSF experimental group were significantly lower than their respective pretreatment groups and control experimental group. The LH pulse amplitude and mean LH levels of the treatment group for the Ucn3 optic stimulation 10Hz + aCSF experimental group were also significantly lower than the treatment groups for all other experimental groups presented in Table 1. n = 5-9 per group.

Abbreviations: BIC, bicuculline; LH, luteinizing hormone; MePD, medial amygdala; Ucn3, urocortin-3.

<sup>a</sup>P < .05.

neurons from AAV-injected Ucn3-cre-tdTomato mice revealed that 87.00 ± 6.00% of MePD Ucn3 neurons expressed AAV-ChR2 and the numbers of tdTomato-labeled Ucn3 neurons per side per slice in the MePD were counted at 49.00 ± 5.37 (mean ± SEM) with the number of AAV-ChR2 infected neurons being 43.01 ± 3.65 (mean ± SEM) (n = 8). Nonspecific expression of ChR2 in the MePD (YFP single labeling) has been quantified to be limited to 6 ± 4.63 (mean ± SEM) in all 8 mice. A representative example is shown in Fig. 4A-4F. The optofluid cannula was also verified to be correctly positioned in the MePD in all 8 mice. Evaluation of AAV9-EF1a-double floxed-hChR2(H134R)-EYFP-WPRE-HGHpA expression in Ucn3 projections from the MePD to the PVN showed YFP-labeled fibers in the PVN (Fig. 5, A-Aiii). Local Ucn3 neurons in the PVN are labeled with tdTomato. We cannot however exclude the possibility that a small portion of fibers may

be present that are not colocalized with tdTomato, which may reflect unspecific expression of ChR2 in nerve terminals other than Ucn3 in the PVN. The optic fiber cannula was also verified to be correctly positioned in the PVN in all 8 mice.

## Discussion

We show optogenetic stimulation of MePD Ucn3 neurons inhibits pulsatile LH secretion, an effect that was completely blocked by intra-MePD GABA and glutamate antagonism. Moreover, optogenetic stimulation of MePD Ucn3 projections in the hypothalamic PVN also suppresses LH pulsatility while inducing the release of CORT. These results demonstrate that inhibition of the GnRH pulse generator by Ucn3 neurons within the MePD relies on GABA and glutamate signaling in the MePD, per se. Moreover, MePD Ucn3 efferent projections in the PVN modulate the activity of the HPA and HPG axes.

The MePD is a major upstream regulator of gonadotropic hormone secretion with a significant population of GABAergic neurons projecting to reproductive neural centers in the hypothalamus (29). Although classic lesioning studies suggest an inhibitory output of the MePD over reproductive function (30, 31), selective optical stimulation of MePD kiss1 neurons increases LH pulse frequency (3), which our unpublished observations show relies upon both GABA and glutamate signaling in the MePD. Due to this interesting dichotomy, we have proposed a disinhibitory system, which is consistent with the pallidal origin of this limbic structure (32), whereby MePD kiss1 activation excites inhibitory GABAergic interneurons, which in turn reduces the inhibitory tone of the GABAergic projections from the MePD to the ARC KNDy network allowing for an increase in GnRH pulse generator frequency (3). Contrastingly, kiss1R antagonism, reducing MePD kiss1 signaling, decreases GnRH pulse generator frequency (33).

We have recently shown that stress-induced activation of Ucn3 and CRFR2 signaling within the MePD inhibits GnRH pulse generator activity (4) and activation of MePD Ucn3 neurons delays pubertal timing (34). It has also been

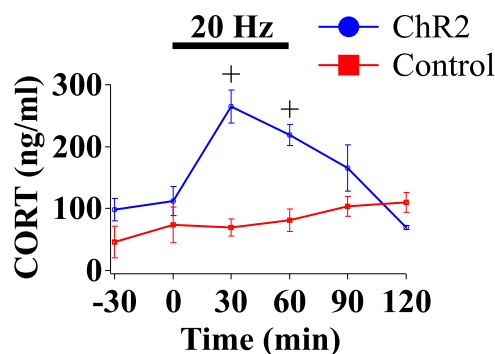


**Figure 2.** Optogenetic stimulation of posterodorsal medial amygdala urocortin-3 neuronal terminals in the hypothalamic paraventricular nucleus with blue light at 20 Hz, 15 mW elevated corticosterone (CORT) secretion in adult ovariectomized + 17β-estradiol Ucn3-cre-tdTomato female mice. CORT secretion time-course for mice receiving optical stimulation initiated at 0 minutes and terminated at 60 minutes (1 hour duration), followed by a 1 hour recovery period (60-120 minutes) for the AAV-ChR2 group (circles) and control group (squares). +P < .05 AAV-ChR2 (n = 6) at time point 30 minutes and 60 minutes vs control (AAV-YFP: n = 5) at time point 30 minutes and 60 minutes.

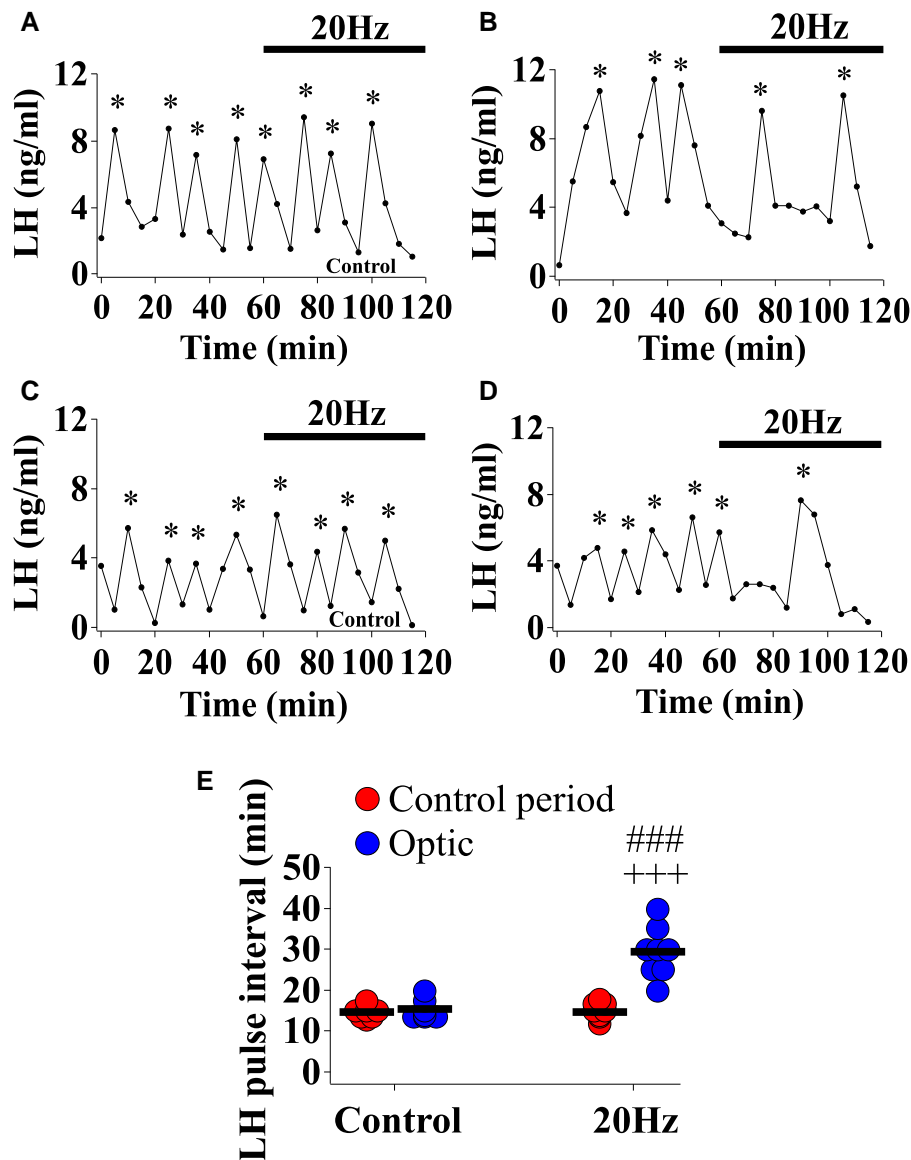


**Figure 3.** Optogenetic stimulation of posterodorsal medial amygdala urocortin-3 neuronal terminals in the hypothalamic paraventricular nucleus with blue light at 20 Hz, 15 mW reduced LH pulsatility in adult ovariectomized + 17 $\beta$ -estradiol Ucn3-cre-tdTomato female mice. Representative LH pulse profiles showing the effects of (A) AAV-YFP/WT mice receiving optical stimulation of 20 Hz, 5 mW, (B) AAV-ChR2 mice receiving optical stimulation of 20 Hz, 5 mW, (C) another example of AAV-YFP/WT mice receiving optical stimulation of 20 Hz, 5 mW, (D) another example of AAV-ChR2 mice receiving optical stimulation of 20 Hz, 5 mW. (E) Summary of LH pulse interval for the prestimulation control period (1 hour) and optic stimulation period (1 hour). LH pulses detected by the DynPeak algorithm are indicated with an asterisk located above each pulse on the representative LH pulse profiles. +++ $P$  < .0001 control period vs optic stimulation for AAV-ChR2 mice ( $n$  = 8); ### $P$  < .0001 AAV-YFP/WT (AAV-YFP,  $n$  = 3; wild-type with AAV-ChR2,  $n$  = 2; no stimulation,  $n$  = 2) vs AAV-ChR2 mice during optic stimulation.

shown that the majority of MePD CRFR2 expressing neurons are GABAergic (21). In the MePD, Ucn3 fibers overlap with sites expressing its cognate receptor CRFR2 (35, 36), and some local Ucn3 neurons within the MePD are shown to have an interneuron-like appearance (37), thus Ucn3 neurons may form connections with and signal via GABAergic CRFR2-positive neurons in this region. In the present study, we show that optogenetic activation of MePD Ucn3 neurons inhibits pulsatile LH secretion. Therefore, we propose that activated MePD Ucn3 neurons may signal through inhibitory GABAergic CRFR2-positive interneurons, upstream of the MePD kiss1 neurons, downregulating MePD kiss1 signaling and resulting in decreased GnRH pulse generator frequency, as illustrated in Fig. 6A.

In our proposed model, we hypothesized that GABA signaling is an important factor mediating the suppressive effect of MePD Ucn3 activation on GnRH pulse generator activity. Therefore, we tested the effect of intra-MePD administration of GABA<sub>A</sub> or GABA<sub>B</sub> receptor antagonists during optical stimulation of MePD Ucn3 neurons on LH pulsatility, and, indeed, we found that both GABA<sub>A</sub> and GABA<sub>B</sub> receptor antagonism blocks the suppression of LH pulses by MePD Ucn3 neuronal activation. Indeed, it has been shown that in GABA<sub>B</sub> receptor knockout mice Kiss1 mRNA expression increases in the MePD, suggesting that GABA<sub>B</sub> regulates Kiss1 expression in this region (38). Whether the MePD kiss1 neurons also contain GABA<sub>A</sub> receptors is unknown. Selective optical stimulation of Ucn3 neurons may activate inhibitory

**Table 2. LH pulse amplitude and mean LH levels before and during optogenetic stimulation of Ucn3 projection neurons in the hypothalamic PVN originating from the posterodorsal subnucleus of the MePD in OVX Ucn3-cre-tdTomato female mice replaced with 17 $\beta$ -estradiol capsules**

Treatment	Mean LH pulse amplitude (ng/mL)		Mean LH level (ng/mL)	
	Pretreatment	Treatment	Pretreatment	Treatment
Control	5.11 $\pm$ 0.82 <sup>a</sup>	4.86 $\pm$ 0.93	4.03 $\pm$ 0.58 <sup>a</sup>	3.62 $\pm$ 0.50
Ucn3 optic stimulation 20 Hz	5.19 $\pm$ 0.95 <sup>a</sup>	4.01 $\pm$ 0.73	4.73 $\pm$ 0.48	3.13 $\pm$ 0.57

Data are presented as mean  $\pm$  SEM. The LH pulse amplitude of the pretreatment group for the control and Ucn3 optic stimulation 20 Hz experimental groups from Table 2 were significantly lower than pretreatment groups from Table 1 for the Control, Ucn3 optic stimulation 10Hz + aCSF, CGP, and Ucn3 optic stimulation 10Hz + CGP experimental groups. The mean LH levels of the pretreatment group for the Control experimental group from Table 2 were significantly lower than pretreatment groups from Table 1 for the control, Ucn3 optic stimulation 10Hz + aCSF and Ucn3 optic stimulation 10Hz + CGP experimental groups. n = 6-8 per group.

Abbreviations: aCSF, artificial cerebrospinal fluid; LH, luteinizing hormone; MePD, medial amygdala; OVX, ovariectomized; PVN, paraventricular nucleus; Ucn3, urocortin-3.

<sup>a</sup>P < .05

GABAergic CRFR2-positive interneurons (38), which in turn downregulate MePD kiss1 signaling, which we have previously shown results in suppression of GnRH pulse generator frequency (33) (see Fig. 6A). However, based on our proposed neuronal circuit, GABA<sub>A</sub> and GABA<sub>B</sub> receptor antagonism may be working upstream and downstream of MePD kiss1 activity to cancel both the inhibitory GABAergic CRFR2 interneurons upstream of and the inhibitory GABAergic interneurons downstream of MePD kiss1 neurons. Therefore, the inhibitory output of the MePD GABAergic projection neurons to the ARC KNDy network is cancelled, thus negating the suppressive effect of MePD Ucn3 activation on the GnRH pulse generator, and, essentially, terminating the ability of the GABA interneuron, upstream and downstream of MePD kiss1 activity, to take part in the disinhibition by antagonizing GABA receptors located on the MePD kiss1 neurons as well as postsynaptic GABA projection neurons removing the inhibitory control over the GnRH pulse generator from the MePD (see Fig. 6B).

We have identified GABA signaling as a key part of the MePD Ucn3 neural circuitry associated with suppression of

the GnRH pulse generator; however, glutamate signaling in the amygdala is also known to be involved in modulating reproduction and anxiety-like behavior (39). Administration of NMDA into the MePD disrupts ovarian cycles in rats, while NMDA receptor antagonism in the MePD delays pubertal timing (31). We hypothesized that glutamate neurotransmission may form a critical part of the MePD Ucn3 neural circuitry involved in stress-induced inhibition of GnRH pulse generator activity. In the present study, we show that intra-MePD AMPA and NMDA receptor antagonism blocks the inhibitory effect of MePD Ucn3 neuronal activation on LH pulsatility. These observations suggest the involvement of neural circuitry similar to that in the neighboring posteroventral medial amygdala, which exhibits functional glutamatergic signaling onto inhibitory GABA neurons (32). Moreover, inhibition of both GABA and glutamate signaling is equally effective at blocking suppression of LH pulses, suggesting they are key components in the circuit.

We know the MePD Ucn3 neurons are interconnected with each other and CRFR2 expressing neurons, forming a Ucn3-CRFR2 neuronal circuit (21). The effect of glutamate

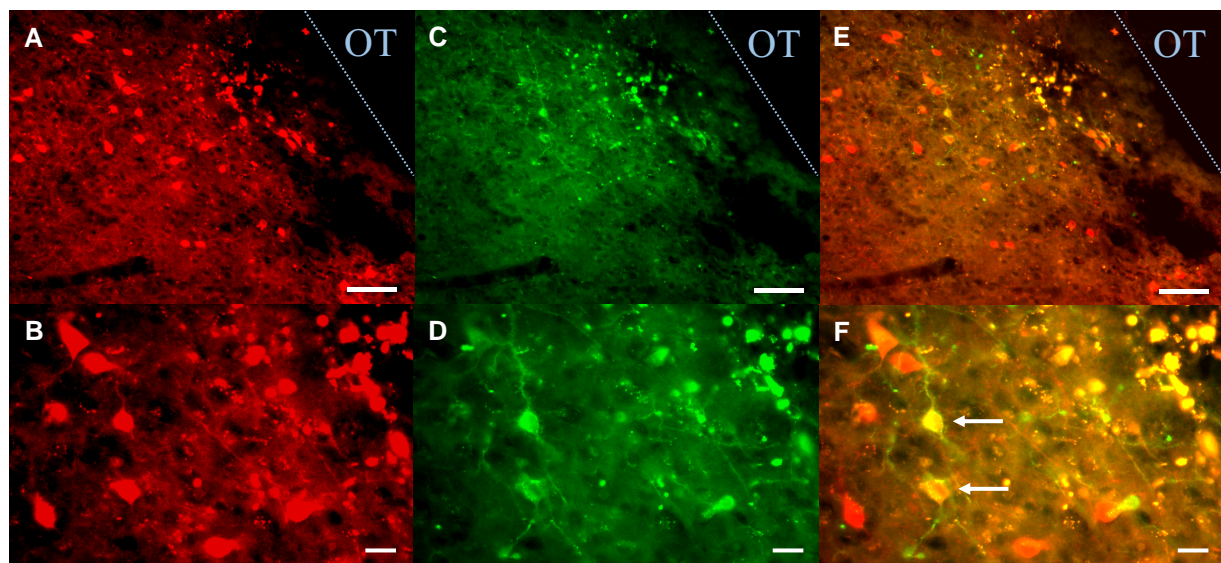


**Figure 4.** Expression of AAV9-EF1a-double floxed-hChR2(H134R)-EYFP-WPRE-HGHpA in posterodorsal medial amygdala (MePD) urocortin-3 (Ucn3) neurons. (A-E) Representative dual fluorescence photomicrographs of the MePD from a Ucn3-cre-tdTomato female ovariectomized mouse injected with AAV9-EF1a-double floxed-hChR2(H134R)-EYFP-WPRE-HGHpA. Ucn3 neurons labeled with tdTomato (A) and YFP (C) appear yellow/orange (E). B, D, and F are a higher power view of A, C, and E respectively. Scale bars represent A, C, E, 50  $\mu$ m; and B, D, F 20  $\mu$ m. Arrows show examples of Ucn3 neurons labeled with tdTomato and YFP. OT, optic tract (line).

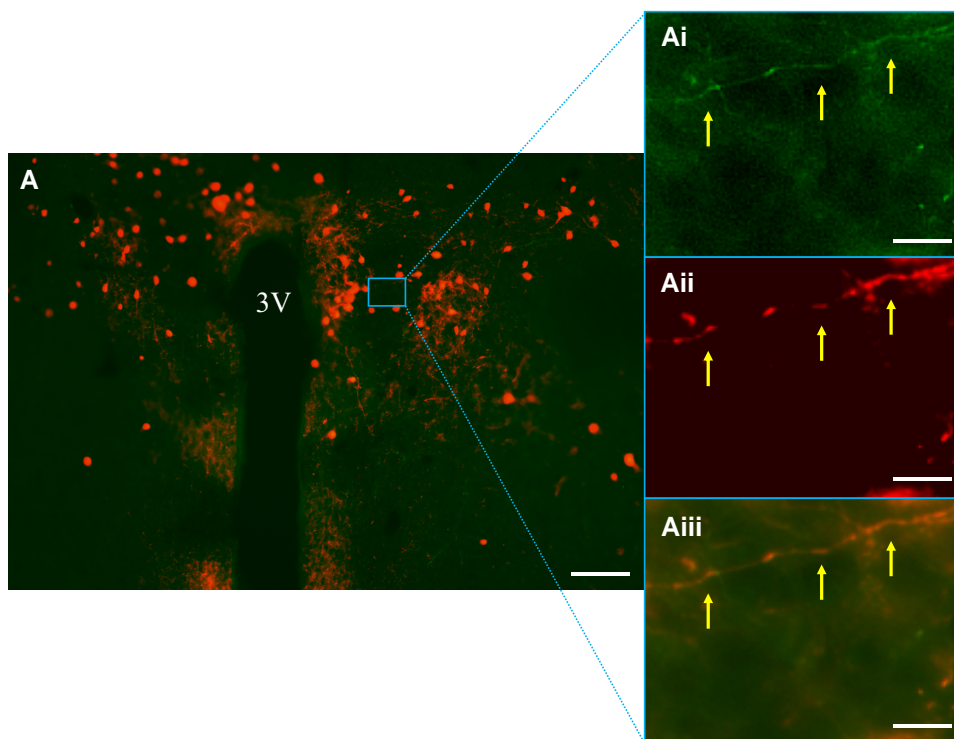


**Figure 5.** Expression of AAV9-EF1a-double floxed-hChR2(H134R)-EYFP-WPRE-HGHpA in urocortin-3 (Ucn3) neuronal projection in the paraventricular nucleus of the hypothalamus (PVN) originating from the posterodorsal medial amygdala. (Ai-Aiii) Representative dual fluorescence photomicrographs of the PVN from a Ucn3-cre-tdTomato female ovariectomized + 17 $\beta$ -estradiol mouse injected with AAV9-EF1a-double floxed-hChR2(H134R)-EYFP-WPRE-HGHpA. Ucn3 neurons and projections labeled with (A) YFP and tdTomato expression in PVN; (Ai) higher power view of YFP labeled MePD Ucn3 projections in the PVN; (Aii) higher power view of tdTomato labeled MePD Ucn3 projections in the PVN; and (Aiii) YFP and tdTomato merged. Scale bars: A, 100  $\mu$ m; Ai, Aii, and Aiii, 10  $\mu$ m. Box shows the YFP-labeled MePD Ucn3 projection in the PVN, arrows point to parts of the YFP-labeled MePD Ucn3 projection in the PVN. 3V, third ventricle.

antagonism, illustrated in Fig. 6C, suggests that glutamate transmission may be mediated via glutamatergic Ucn3 neurons. This has been shown in the hypothalamic perifornical area, where they are activated during infant-directed aggression (40) and increase anxiety-like behavior (41), but this awaits future study for the MePD Ucn3 neuronal population. Our previous data have shown that infusing Ucn3 in the MePD blocks LH pulses, indicating their activity in this brain region is sufficient to suppress GnRH pulse generator activity (4). We have also shown that infusion of CRFR2 antagonists in the MePD blocks the stress-induced suppression of LH pulses, suggesting MePD CRFR2-expressing neurons are also involved in modulating the GnRH pulse generator under stressful conditions. Our current data expand on our previous observations determining whether neurotransmission modulating pulsatile LH secretion is involved in this MePD circuit. Our results suggest that glutamate may be necessary for the inhibition of LH pulses induced by activation of MePD Ucn3 neurons, thus we show that glutamate signaling is an indispensable part of this circuit. Based on our observations, we propose that Ucn3 neurons in the MePD may be glutamatergic, similarly to the Ucn3 neurons in the hypothalamic perifornical area. Glutamate is possibly required to trigger network activity of the MePD Ucn3 neurons similar to the role glutamate plays in the ARC KNDy network (13). This allows the network to reach a certain level of excitability that promotes signaling via Ucn3 to activate CRFR2-expressing GABAergic neurons, which in turn downregulate MePD kiss1 activity, resulting in suppression of GnRH pulse

generator activity. Thus, NMDA and AMPA receptor antagonism possibly cancels MePD Ucn3 glutamatergic activation of inhibitory GABAergic CRFR2-expressing interneurons preventing the decrease in GnRH pulse generator activity (Fig. 6C). However, fast synaptic activity occurs due to synaptic neurotransmitter release, and modulation of this activity is known to be a key target for neuropeptides. Indeed, urocortins can also function endogenously as modulators of excitatory glutamatergic transmission in the amygdala, with *in vitro* studies showing modulation of glutamatergic excitatory postsynaptic potentials via presynaptic and postsynaptic CRFR2-mediated mechanisms (42). Therefore, we cannot exclude the possibility that Ucn3 activity in the MePD is augmenting glutamatergic transmission to activate downstream inhibitory GABA neurons.

The fact that GABAergic and glutamatergic receptor antagonism within the MePD did not alter LH pulsatility without optogenetic stimulation of Ucn3 neurons is an important factor in our proposed mechanisms and neural circuits within the MePD. This observation indicates that under basal nonstress conditions MePD Ucn3 neurons are relatively quiescent; thus solely pharmacologically blocking the upstream GABA and glutamate inputs to the GABAergic MePD projections without a corresponding increase in Ucn3 activity would make little difference to the net effect of the MePD over the KNDy neuronal system.

Stress elevates Ucn3 mRNA (19) and *c-fos* expression in the MePD (18) while chemogenetic inhibition of MePD Ucn3 neurons prevents stress-induced suppression of LH pulsatility (4). The MePD sends stress-activated efferents to the PVN

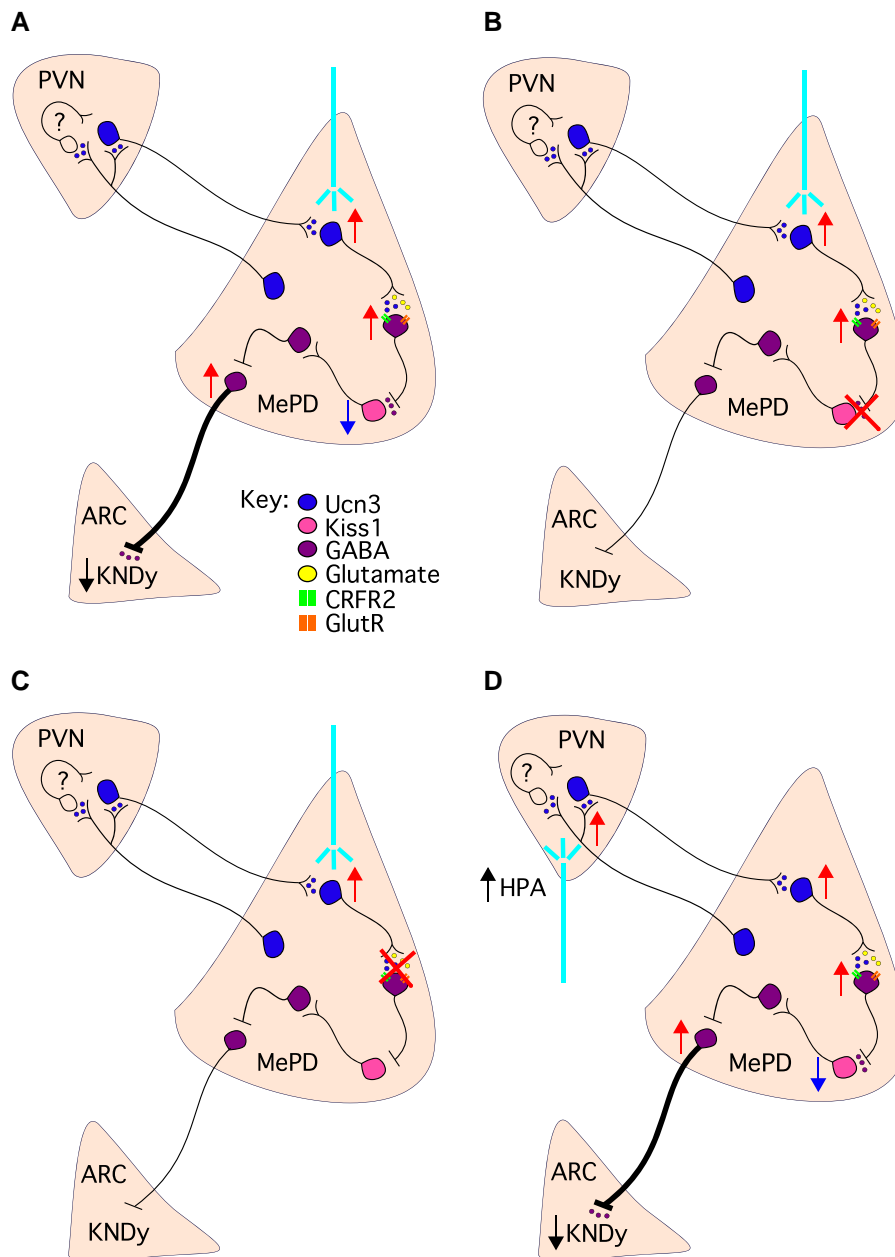


**Figure 6.** Schematic illustration of the proposed model of the MePD neurocircuits and their pharmacological manipulation. (A) Optical stimulation of local MePD Ucn3 neurons releases Ucn3 and the cotransmitter glutamate, which activate inhibitory GABAergic CRFR2-positive interneurons located upstream of the kiss1 neurons suppressing their activity. The reduced kiss1 signaling deactivates its downstream inhibitory GABAergic interneuron causing disinhibition of the GABAergic projection efferents from the MePD, resulting in an increased inhibitory tone over the ARC KNDy network, thus decreasing GnRH pulse generator frequency. (B) Antagonism of both GABA<sub>A</sub> and GABA<sub>B</sub> receptors in the MePD during optical stimulation of Ucn3 neurons blocks the downregulation of kiss1 neuronal activity, preventing the inhibitory effect of Ucn3 signaling on the KNDy network. (C) Antagonism of both NMDA and AMPA receptors in the MePD during optical stimulation of Ucn3 neurons blocks the activation of the downstream GABAergic CRFR2-positive interneurons, preventing the inhibitory effect of Ucn3 signaling on the KNDy network and suggesting glutamate is necessary for the inhibition of pulsatile LH secretion. (D) High-frequency photoactivation of MePD Ucn3 projection terminals in the PVN may activate Ucn3 neurons and/or other neurons of an unknown phenotype in the PVN resulting in stimulation of the HPA axis and CORT release. Additionally, there may be collateral activation of reciprocal PVN Ucn3 projections to the MePD, which in turn relay via the MePD Ucn3 neuronal circuitry an inhibitory influence on the ARC KNDy neuronal network to suppress GnRH pulse generator frequency. Ucn3, urocortin3; CRFR2, corticotropin-releasing factor type 2 receptor; GlutR, glutamate receptor; MePD, posterodorsal subnucleus of the medial amygdala; PVN, paraventricular nucleus of hypothalamus; ARC, hypothalamic arcuate nucleus.

(18), and MePD Ucn3 neurons have been shown to project directly to the PVN (21). In the current study, we demonstrate for the first time that optical stimulation of MePD Ucn3 projections in the PVN inhibits pulsatile LH secretion. Recently, chemogenetic activation of PVN CRF neuron perikarya was shown to rapidly suppress LH pulse frequency; however, optogenetic activation

of their nerve terminals in the ARC does not affect the firing of KNDy neurons (43) and directly injecting CRF in the ARC also has no effect on LH secretion (44), suggesting the involvement of an indirect mechanism inhibiting GnRH pulse generator activity. The MePD has been shown to send Ucn3 neuronal projections to the PVN and receive Ucn3 projections from the PVN,

indicating bidirectional communication between these 2 brain regions via Ucn3 signaling (21). Moreover, the MePD sends direct efferent projections to KNDy neurons of an unknown neurochemical phenotype (8). Therefore, stressful stimuli may be processed by PVN CRF or Ucn3 neurons and this information may be relayed via the MePD Ucn3 neuronal circuitry to the ARC KNDy neurons to modulate their activity (see Fig. 6D). Ultimately, the MePD may function as a novel relay center between the PVN and ARC to regulate stress signals to the GnRH pulse generator and contribute to the crosstalk between the reproductive and stress axes.

Central administration of Ucn3 augments the HPA axis response to restraint stress in rats (19) and increases hypothalamic CRF concentrations and circulating levels of CORT in mice (45). Overexpression of Ucn3 in the hypothalamic perifornical area increases anxiety-like behavior (41), and activation of the CRFR2 in the lateral septum is involved in stress-induced persistent anxiety in mice (46). In the medial amygdala, Ucn3 neuronal populations are shown to consist of both projection neurons extending to the PVN, the bed nucleus of the stria terminalis, and the suprachiasmatic nucleus (21, 37) and local Ucn3 interneurons (35, 36). We have previously shown chemogenetic inhibition targeting both local and efferent MePD Ucn3 neurons prevents psychosocial stress-induced release of CORT (4). In the present study, we show that selective optogenetic activation of MePD Ucn3 projections in the PVN elevates CORT secretion, thus MePD Ucn3 projections to the PVN are critical for the regulation of CORT secretion. Further work is required to identify whether only the MePD Ucn3 projecting efferents to the PVN are crucial for regulating CORT secretion. The presence of E<sub>2</sub> is known to upregulate basal CRF mRNA levels in the PVN in rodents and induce high levels of circulating CORT providing a sensitizing effect to the activity of the HPA axis (23, 24). Moreover, the CRFR2 promoter contains a classical estrogen receptor response element (47), indicating that CRFR2 activity is upregulated in the presence of E<sub>2</sub>. Therefore, we implanted the OVX mice with E<sub>2</sub> capsules for HPA axis sensitization in mice similarly to what has been reported in previous studies (23, 25, 26, 48). However, E<sub>2</sub> levels may have fallen lower than expected, to low or potentially below the physiological range observed in diestrous mice, as evidenced by little or no effect on LH pulse frequency. However, an effect on LH pulse amplitude and mean LH levels was evident in the E<sub>2</sub> replaced animals. Although there was weak E<sub>2</sub> negative feedback on LH pulses in our model, our main reason for E<sub>2</sub> replacement was to sensitize the HPA axis (23, 25, 26, 48). PVN-CRF neurons express mRNA transcripts for CRFR2 (49) and CRFR2 primarily activate the G<sub>αs</sub> adenylyl cyclase/cAMP signaling pathway (50), indicating that signaling via the CRFR2 located on PVN-CRF neurons may result in activation of this neuronal population and hence the HPA axis (see Fig. 6D). Therefore, Ucn3 released following optical stimulation of MePD Ucn3 projections in the PVN may directly activate the PVN-CRF neurons, signaling via CRFR2, to stimulate CORT release as observed in the present study. However, this hypothesis requires further experimental interrogation.

Selective CRFR2 antagonism has been shown to reverse the stress-induced inhibition of LH pulses (51) where central administration of astressin2-B, a specific CRFR2 antagonist, blocked the restraint-stress-induced suppression of pulsatile LH secretion in rats (52). We have shown specific antagonism

of CRFR2 in the MePD blocked the inhibitory effects of predator odor on the GnRH pulse generator in mice (4) and activation of MePD Ucn3 neurons delayed puberty in mice (34). Therefore, we know CRFR2 neurons are involved in processing stressful information and coordinating the activity of the GnRH pulse generator accordingly. Additionally, CRF is also implicated in reducing pulsatile LH secretion via CRFR1 expressing neurons in mice (53). Chronic stress levels of CORT decrease LH pulsatility (54) and recently an acute rise in CORT sustained for 30 to 60 minutes was shown to inhibit pulsatile LH release, but only in OVX mice with estrogen replacement (55) and after a delay of approximately 30 minutes following the CORT rise. From our observations, inhibition of LH pulsatility occurs immediately after the stimulation of MePD Ucn3 projections in the PVN in OVX E<sub>2</sub> replaced mice, thus it is unlikely the result of negative feedback from CORT release but rather a central suppression of GnRH pulse generator activity possibly from the activation of PVN CRF neurons, although the mechanism involved has yet to be established. Moreover, acute psychosocial stress exposure reduces LH pulse frequency in OVX mice (4, 56), suggesting E<sub>2</sub> is not necessary for the inhibition of the GnRH pulse generator in response to psychosocial stress (4, 56). Therefore, acute stress pathways possibly act via CORT and E<sub>2</sub> independent pathways to suppress LH pulses. In our study, optical stimulation of MePD Ucn3 local and efferent neurons is supposed to mimic acute exposure to psychosocial stress as this has been shown to be processed by Ucn3 activity in the MePD, thus supporting the idea of a central suppression of GnRH pulse generator activity mediated by MePD Ucn3 neurons.

The PVN CRF neuronal population was not traditionally considered important for mediating stress-induced suppression of pulsatile LH secretion, as PVN lesion studies have shown that this region is not critical in mediating the stress-induced suppression of the reproductive axis (57). However, with the recent observations showing that chemogenetic activation of PVN CRF neurons indirectly inhibits the GnRH pulse generator it is plausible that the stress neural circuitry includes upstream signaling via the MePD. Therefore, a possible route may involve stressful information processed by the PVN CRF neurons relayed via the MePD Ucn3 neuronal circuitry to the ARC KNDy neurons to modulate their activity (see Fig. 6D). The neighboring central nucleus of the amygdala is known to act as a relay center in pain control where the central lateral part receives nociceptive input from the parabrachial nucleus and the central medial part is involved in regulating the output of defensive behavior and nociception (58). Local and efferent MePD Ucn3 signaling plays a critical dual role in regulating GnRH pulse generator activity and CORT secretion, thus MePD Ucn3 neuronal populations and their projections may represent a novel nodal center in the interaction between the reproductive and stress axes.

Our findings show for the first time that stimulation of local Ucn3 neurons in the MePD inhibits GnRH pulse generator activity involving an interplay between Ucn3, GABA, and glutamate signaling within the MePD. Furthermore, we interrogate the MePD Ucn3 neuron projection terminals in the PVN, demonstrating that stimulation of the MePD Ucn3 efferent projections in the PVN elevates CORT secretion to stress levels while suppressing the GnRH pulse generator. How the local neural circuit within the MePD engages with efferent projections from the MePD to the PVN and the interplay between

Ucn3, GABA, and glutamate neurons to mediate the suppressive effect on LH pulsatility and the stimulatory effect on the HPA axis remains an exciting question for the future.

## Funding

The authors gratefully acknowledge the financial support from UKRI: UKRI: BBSRC (BB/S000550/1 and BB/W005913/1). D.I. is a PhD student funded by the MRC.

## Disclosures

The authors declare no competing financial interests.

## Data Availability

Some or all data generated or analyzed during this study are included in this published article or in the data repositories listed in References.

## References

- Ressler KJ. Amygdala activity, fear, and anxiety: modulation by stress. *Biol Psychiatry*. 2010;67(12):1117-1119.
- Lin Y, Li XF, Lupi M, et al. The role of the medial and central amygdala in stress-induced suppression of pulsatile LH secretion in female rats. *Endocrinology*. 2011;152(2):545-555.
- Lass G, Li XF, de Burgh RA, et al. Optogenetic stimulation of kisspeptin neurones within the posterodorsal medial amygdala increases luteinising hormone pulse frequency in female mice. *J Neuroendocrinol*. 2020;32(2):e12823.
- Ivanova D, Li XF, McIntyre C, Liu Y, Kong L, O'Byrne KT. Urocortin3 in the posterodorsal medial amygdala mediates stress-induced suppression of LH pulsatility in female mice. *Endocrinology*. 2021;162(12):bqab206.
- Adekunbi DA, Li XF, Li S, et al. Role of amygdala kisspeptin in pubertal timing in female rats. *PLoS One*. 2017;12(8):e0183596.
- Li XF, Adekunbi DA, Alobaid HM, et al. Role of the posterodorsal medial amygdala in predator odour stress-induced puberty delay in female rats. *J Neuroendocrinol*. 2019;31(6):e12719.
- Moore AM, Coolen LM, Lehman MN. Kisspeptin/Neurokinin B/Dynorphin (KNDy) cells as integrators of diverse internal and external cues: evidence from viral-based monosynaptic tract-tracing in mice. *Sci Rep*. 2019;9(1):1-5.
- Yeo SH, Kyle V, Blouet C, Jones S, Colledge WH. Mapping neuronal inputs to Kiss1 neurons in the arcuate nucleus of the mouse. *PLoS One*. 2019;14(3):e0213927.
- Clarkson J, Han SY, Piet R, et al. Definition of the hypothalamic GnRH pulse generator in mice. *Proc Natl Acad Sci U S A*. 2017;114(47):e10216-23.
- Qiu J, Nestor CC, Zhang C, et al. High-frequency stimulation-induced peptide release synchronizes arcuate kisspeptin neurons and excites GnRH neurons. *Elife*. 2016;5:e16246.
- Voliotis M, Li XF, De Burgh R, et al. The origin of GnRH pulse generation: an integrative mathematical-experimental approach. *J Neurosci*. 2019;39(49):9738-9747.
- Moore AM, Coolen LM, Lehman MN. In vivo imaging of the GnRH pulse generator reveals a temporal order of neuronal activation and synchronization during each pulse. *Proc Natl Acad Sci U S A*. 2022;119(6):e2117767119.
- Voliotis M, Li XF, De Burgh RA, et al. Modulation of pulsatile GnRH dynamics across the ovarian cycle via changes in the network excitability and basal activity of the arcuate kisspeptin network. *Elife*. 2021;10:e71252.
- Han SY, McLennan T, Czielesky K, Herbison AE. Selective optogenetic activation of arcuate kisspeptin neurons generates pulsatile luteinizing hormone secretion. *Proc Natl Acad Sci U S A*. 2015;112(42):13109-13114.
- Martin EI, Ressler KJ, Binder E, Nemeroff CB. The neurobiology of anxiety disorders: brain imaging, genetics, and psychoneuroendocrinology. *Psychiatr Clin North Am*. 2009;32(3):549-575.
- Nuss P. Anxiety disorders and GABA neurotransmission: A disturbance of modulation. *Neuropsychiatr Dis Treat*. 2015;11:165-175.
- Takahashi LK. Olfactory systems and neural circuits that modulate predator odor fear. *Front Behav Neurosci*. 2014;8:72.
- Van-Hover C, Li C. Stress-activated afferent inputs into the anterior parvocellular part of the paraventricular nucleus of the hypothalamus: insights into urocortin 3 neuron activation. *Brain Res*. 2015;1611:29-43.
- Jamieson PM, Li C, Kukura C, Vaughan J, Vale W. Urocortin 3 modulates the neuroendocrine stress response and is regulated in rat amygdala and hypothalamus by stress and glucocorticoids. *Endocrinology*. 2006;147(10):4578-4588.
- Fekete EM, Zhao Y, Li C, Sabino V, Vale WW, Zorrilla EP. Social defeat stress activates medial amygdala cells that express type 2 corticotropin-releasing factor receptor mRNA. *Neuroscience*. 2009;162(1):5-13.
- Shemesh Y, Forkosh O, Mahn M, et al. Ucn3 and CRF-R2 in the medial amygdala regulate complex social dynamics. *Nat Neurosci*. 2016;19(11):1489-1496.
- Ingberg E, Theodorsson A, Theodorsson E, Strom JO. Methods for long-term 17 $\beta$ -estradiol administration to mice. *Gen Comp Endocrinol*. 2012;175(1):188-193.
- Li XF, Mitchell JC, Wood S, Coen CW, Lightman SL, O'Byrne KT. The effect of oestradiol and progesterone on hypoglycaemic stress-induced suppression of pulsatile luteinizing hormone release and on corticotropin-releasing hormone mRNA expression in the rat. *J Neuroendocrinol*. 2003;15(5):468-476.
- Zavala E, Voliotis M, Zerenner T, et al. Dynamic hormone control of stress and fertility. *Front Physiol*. 2020;11:1457.
- Chen MD, O'Byrne KT, Chiappini SE, Hotchkiss J, Knobil E. Hypoglycemic "stress" and gonadotropin-releasing hormone pulse generator activity in the rhesus monkey: role of the ovary. *Neuroendocrinology*. 1992;56(5):666-673.
- Cagampang FR, Cates PS, Sandhu S, et al. Hypoglycaemia-induced inhibition of pulsatile luteinizing hormone secretion in female rats: role of oestradiol, endogenous opioids and the adrenal medulla. *J Neuroendocrinol*. 1997;9(11):867-872.
- Paxinos G, Franklin KB. *Mouse brain in stereotaxic coordinates*. Acad Press. 2019; 5:246.
- McCosh RB, Kreisman MJ, Breen KM. Frequent tail-tip blood sampling in mice for the assessment of pulsatile luteinizing hormone secretion. *J Vis Exp*. 2018;(137):57894.
- Pardo-Bellver C, Cádiz-Moretti B, Novejarque A, Martínez-García F, Lanuza E. Differential efferent projections of the anterior, posterior-ventral, and posterodorsal subdivisions of the medial amygdala in mice. *Front Neuroanat*. 2012;6(33):1-26.
- Stephens SBZ, Raper J, Bachevalier J, Wallen K. Neonatal amygdala lesions advance pubertal timing in female rhesus macaques. *Psychoneuroendocrinology*. 2015;51:307-317.
- Li XF, Hu MH, Hanley BP, et al. The posterodorsal medial amygdala regulates the timing of puberty onset in female rats. *Endocrinology*. 2015;156(10):3725-3736.
- Keshavarzi S, Sullivan RKP, Ianno DJ, Sah P. Functional properties and projections of neurons in the medial amygdala. *J Neurosci*. 2014;34(26):8699-8715.
- Comninos AN, Anastasovska J, Sahuri-Arisoylu M, et al. Kisspeptin signaling in the amygdala modulates reproductive hormone secretion. *Brain Struct Funct*. 2016;221(4):2035-2047.
- Ivanova D, Li X, Liu Y, et al. Role of posterodorsal medial amygdala urocortin-3 in pubertal timing in female mice. *Front Endocrinol (Lausanne)*. 2022;13:893029.
- Cavalcante JC, Sita LV, Mascaro MB, Bittencourt JC, Elias CF. Distribution of urocortin 3 neurons innervating the ventral pre-mammillary nucleus in the rat brain. *Brain Res*. 2006;1089(1):116-125.

36. Li C, Vaughan J, Sawchenko PE, Vale WW. Urocortin III-immunoreactive projections in rat brain: partial overlap with sites of type 2 corticotrophin-releasing factor receptor expression. *J Neurosci.* 2002;22(3):991-1001.
37. Deussing JM, Breu J, Kühne C, et al. Urocortin 3 modulates social discrimination abilities via corticotropin-releasing hormone receptor type 2. *J Neurosci.* 2010;30(27):9103-9116.
38. Di Giorgio NP, Semaan SJ, Kim J, et al. Impaired GABAB receptor signaling dramatically up-regulates Kiss1 expression selectively in nonhypothalamic brain regions of adult but not prepubertal mice. *Endocrinology.* 2014;155(3):1033-1044.
39. Hegoburu C, Parrot S, Ferreira G, Mouly AM. Differential involvement of amygdala and cortical NMDA receptors activation upon encoding in odor fear memory. *Learn Mem.* 2014;21(12):651-655.
40. Autry AE, Wu Z, Kapoor V, et al. Urocortin-3 neurons in the mouse perifornical area promote infant-directed neglect and aggression. *Elife.* 2021;10:e64680.
41. Kuperman Y, Issler O, Regev L, et al. Perifornical urocortin-3 mediates the link between stress-induced anxiety and energy homeostasis. *Proc Natl Acad Sci U S A.* 2010;107(18):8393-8398.
42. Liu J, Yu B, Neugebauer V, et al. Corticotropin-releasing factor and urocortin I modulate excitatory glutamatergic synaptic transmission. *J Neurosci.* 2004;24(16):4020-4029.
43. Yip SH, Liu X, Hessler S, Cheong I, Porteous R, Herbison AE. Indirect suppression of pulsatile LH secretion by CRH neurons in the female mouse. *Endocrinology.* 2021;162(3):bqaa237.
44. Rivest S, Plotsky PM, Rivier C. CRF Alters the infundibular LHRH secretory system from the medial preoptic area of female rats: possible involvement of opioid receptors. *Neuroendocrinology.* 1993;57(2):236-246.
45. Bagosi Z, Csabafi K, Karasz G, et al. The effects of the urocortins on the hypothalamic-pituitary-adrenal axis—similarities and discordances between rats and mice. *Peptides.* 2019;112:1-13.
46. Anthony TE, Dee N, Bernard A, Lerchner W, Heintz N, Anderson DJ. Control of stress-induced persistent anxiety by an extra-amygdala septohypothalamic circuit. *Cell.* 2014;156(3):522-536.
47. Catalano RD, Kyriakou T, Chen J, Easton A, Hillhouse EW. Regulation of corticotropin-releasing hormone type 2 receptors by multiple promoters and alternative splicing: identification of multiple splice variants. *Mol Endocrinol.* 2003;17(3):395-410.
48. McCosh RB, Breen KM, Kauffman AS. Neural and endocrine mechanisms underlying stress-induced suppression of pulsatile LH secretion. *Mol Cell Endocrinol.* 2019;498:110579.
49. Dabrowska J, Hazra R, Guo JD, DeWitt S, Rainnie DG. Central CRF neurons are not created equal: phenotypic differences in CRF-containing neurons of the rat paraventricular hypothalamus and the bed nucleus of the stria terminalis. *Front Neurosci.* 2013;7:156.
50. Deussing JM, Chen A. The corticotropin-releasing factor family: physiology of the stress response. *Physiol Rev.* 2018;98(4):2225-2286.
51. Li XF, Bowe JE, Kinsey-Jones JS, Brain SD, Lightman SL, O'Byrne KT. Differential role of corticotropin-releasing factor receptor types 1 and 2 in stress-induced suppression of pulsatile luteinizing hormone secretion in the female rat. *J Neuroendocrinol.* 2006;18(8):602-610.
52. Li XF, Bowe JE, Lightman SL, O'Byrne KT. Role of corticotropin-releasing factor receptor-2 in stress-induced suppression of pulsatile luteinizing hormone secretion in the rat. *Endocrinology.* 2005;146(1):318-322.
53. Raftogianni A, Roth LC, García-González D, et al. Deciphering the contributions of CRH receptors in the brain and pituitary to stress-induced inhibition of the reproductive axis. *Front Mol Neurosci.* 2018;11:305.
54. Kreisman MJ, McCosh RB, Tian K, Song CI, Breen KM. Estradiol enables chronic corticosterone to inhibit pulsatile luteinizing hormone secretion and suppress Kiss1 neuronal activation in female mice. *Neuroendocrinology.* 2020;110(6):501-516.
55. Kreisman MJ, McCosh RB, Breen KM. Role of CORT duration and estradiol dependence for stress-level of CORT to inhibit pulsatile LH secretion in female mice. *J Endocr Soc.* 2021;5(Suppl 1):A552.
56. Yang JA, Song CI, Hughes JK, et al. Acute psychosocial stress inhibits LH pulsatility and kiss1 neuronal activation in female mice. *Endocrinology.* 2017;158(11):3716-3723.
57. Serge S, Rivier C. Influence of the paraventricular nucleus of the hypothalamus in the alteration of neuroendocrine functions induced by intermittent footshock or interleukin. *Endocrinology.* 1991;129(4):2049-2058.
58. Wank I, Pliota P, Badurek S, et al. Central amygdala circuitry modulates nociceptive processing through differential hierarchical interaction with affective network dynamics. *Commun Biol.* 2021;4(1):1-10.